Longitudinal Splitting of Boron Nitride Nanotubes for the Facile Synthesis of High Quality Boron Nitride Nanoribbons

ARTICLE *in* NANO LETTERS · MAY 2011

Impact Factor: 13.59 · DOI: 10.1021/nl2014857 · Source: PubMed

NANO LETTERS

LETTER

pubs.acs.org/NanoLett

Longitudinal Splitting of Boron Nitride Nanotubes for the Facile Synthesis of High Quality Boron Nitride Nanoribbons

Kris J. Erickson,[†,‡,§] Ashley L. Gibb,[†,‡,§] Alexander Sinitskii,[⊥] Michael Rousseas,[†,§] Nasim Alem,[†,§,∥] James M. Tour,[*,⊥] and Alex K. Zettl[*,†,§]

[†]Department of Physics and [‡]Department of Chemistry, University of California at Berkeley, Berkeley, California 94720, United States

[§]Materials Sciences Division, Lawrence Berkeley National Laboratory, Berkeley, California 94720, United States

[∥]Center of Integrated Nanosystems, University of California at Berkeley, Berkeley, California 94720, United States

[⊥]Department of Chemistry, Department of Mechanical Engineering and Materials Science, and The Smalley Institute for Nanoscale Science and Technology, Rice University, Houston, Texas 77005, United States

Supporting Information

ABSTRACT:

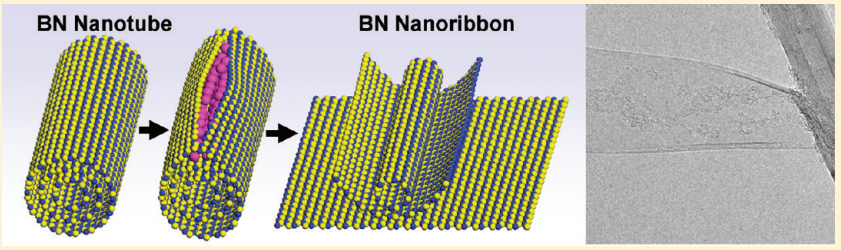

Boron nitride nanoribbons (BNNRs), the boron nitride structural equivalent of graphene nanoribbons (GNRs), are predicted to possess unique electronic and magnetic properties. We report the synthesis of BNNRs through the potassium-intercalation-induced longitudinal splitting of boron nitride nanotubes (BNNTs). This facile, scalable synthesis results in narrow (down to 20 nm), few sheet (typically 2−10), high crystallinity BNNRs with very uniform widths. The BNNRs are at least 1 μm in length with minimal defects within the ribbon plane and along the ribbon edges.

KEYWORDS: Boron nitride, nanomaterials, nanoribbons, splitting, nanotubes

Since the discovery of carbon nanotubes (CNTs),[1] the scientific community has witnessed greatly expanded interest in one- and two-dimensional allotropes of carbon, including graphene[2,3] and graphene nanoribbons (GNRs)[4−7] (Figure 1). Although graphene and GNRs share a common sp^2-bonded carbon framework,[3] the different boundary conditions lead to unique properties. With sp^2-bonded boron nitride, which shares structural analogs with carbon (Figure 1), a similar discovery progression can be mapped from boron nitride nanotubes (BNNTs)[8] to few-layer hexagonal boron nitride (*h*-BN) sheets[9] to a recent mounting interest in boron nitride nanoribbons (BNNRs).[10−19] Significantly different properties also exist between these BN-based materials. For example, BNNRs are theorized to possess a wide range of electronic, optical, and magnetic properties arising from various edge structures and terminations.[12,13,15,17−19] These properties are of great fundamental interest and they also have implications for applications within various fields including spintronics and optoelectronics.[12−14,17−19]

Numerous routes to GNRs are now well established,[4−7] and some of these approaches, such as the plasma etching of nanotubes imbedded within a polymer,[5] have been explored for the syntheses of BNNRs.[18] However, unlike the case for GNRs,[4,6,7] the facile, scalable synthesis of high quality BNNRs remains a significant challenge. A particularly effective route to high quality GNRs involves potassium-intercalation-induced longitudinal splitting of CNTs.[7] This is the approach taken here for the synthesis of BNNRs.

Figure 2 shows pictorially the mechanism for splitting BNNTs through alkali metal intercalation. Using this approach, we find that potassium vapor treatment of BNNTs yields narrow (between 20 and 50 nm), long (at least 1 μm in length), few sheet (usually between 2 and 10 layer) pristine BNNRs with very uniform widths as well as minimal defects within the ribbon plane and along their edges. The synthesis process is bulk, facile, and easily scalable. Approximately 1% of treated BNNTs exhibit splitting, comparable to a common bulk route to GNRs,[4] and separation should be possible through established GNR purification techniques.[4,7] Our process allows for BNNRs that can be stabilized in a solvent and then dispersed onto various substrates to allow for further characterization and potential device fabrication.[20]

Precursor BNNTs were synthesized through a process similar to a previously reported route.[21] A mixture of solid boron, magnesium oxide, and tin oxide powders were placed in a graphite crucible that

Received: May 4, 2011

   dx.doi.org/10.1021/nl2014857 | *Nano Lett.* XXXX, XXX, 000–000

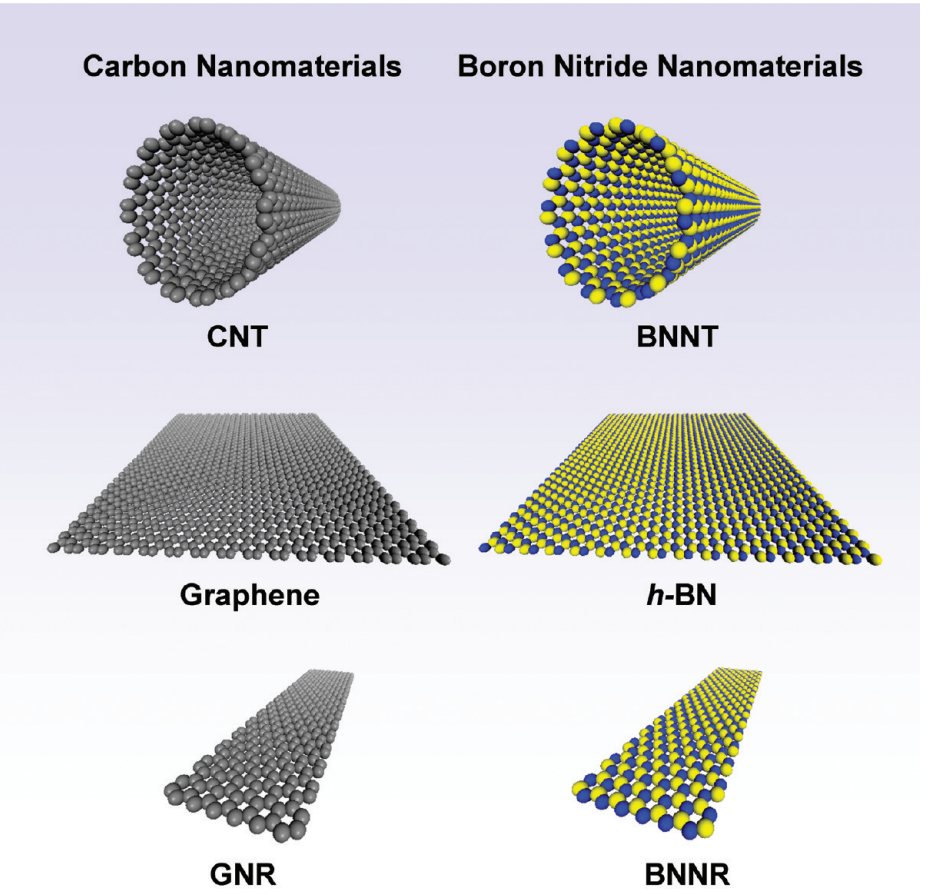

Figure 1. (Left) One and two-dimensional carbon nanomaterials including a CNT, graphene, and a GNR. Carbon atoms are displayed in gray. (Right) One and two-dimensional boron nitride structural analogues including a BNNT, single sheet *h*-BN, and a BNNR. Boron atoms are displayed in blue and nitrogen atoms are displayed in yellow. Though local bonding configurations are nearly identical for the materials in each column, boundary conditions of the selected overall geometries result in unique distinct edge states and unique characteristics. For nanotubes, the circumference defines a boundary condition, whereas for a large nanosheet the circumferential boundary conditions are lifted and edge states have minimal affect. For nanoribbons, the width defines new boundary conditions and edge states can significantly affect many material properties.

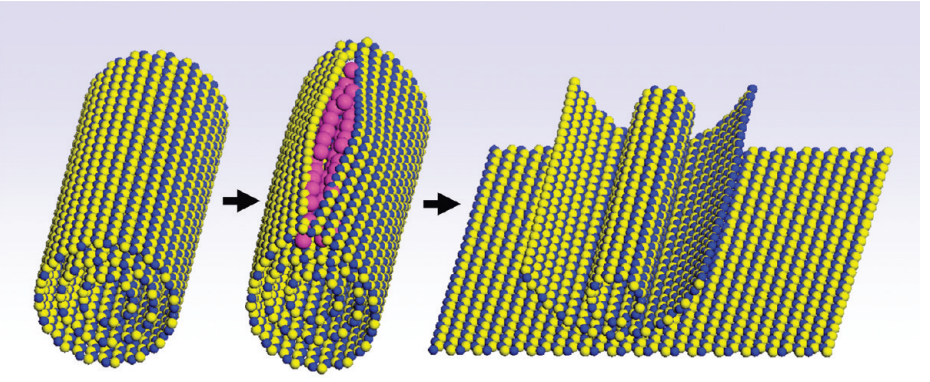

Figure 2. Schematic of the splitting process of a BNNT to form a BNNR. Boron atoms are in blue, nitrogen atoms are in yellow, and potassium atoms are in pink. The pristine BNNT (left) begins to locally unzip owing to potassium intercalation induced pressure buildup (middle), which results in further splitting of the nanotube in the longitudinal direction to form few layer nanoribbons (right).

was heated under a nitrogen atmosphere in a vertical induction furnace to 1500 °C. Nitrogen carrier gas brought the powder into a graphite vessel where it reacted with ammonia to form a white, spongy material rich in BNNTs. BNNTs were taken as-synthesized, placed into an ampule with excess freshly cut potassium metal, evacuated to 10^{-6} Torr, and then heated at 300 °C for 72 h. After removal from the ampule, the material was brought to 600 °C in air for 30 min to remove any carbonaceous impurities. This material was readily dispersed under mild sonication into isopropanol and dried onto lacey carbon TEM grids for analysis.

The synthesized BNNTs were of variable diameters ranging from 6 to 70 nm (see Supporting Information Figure S1).

dx.doi.org/10.1021/nl2014857 |*Nano Lett.* XXXX, XXX, 000–000

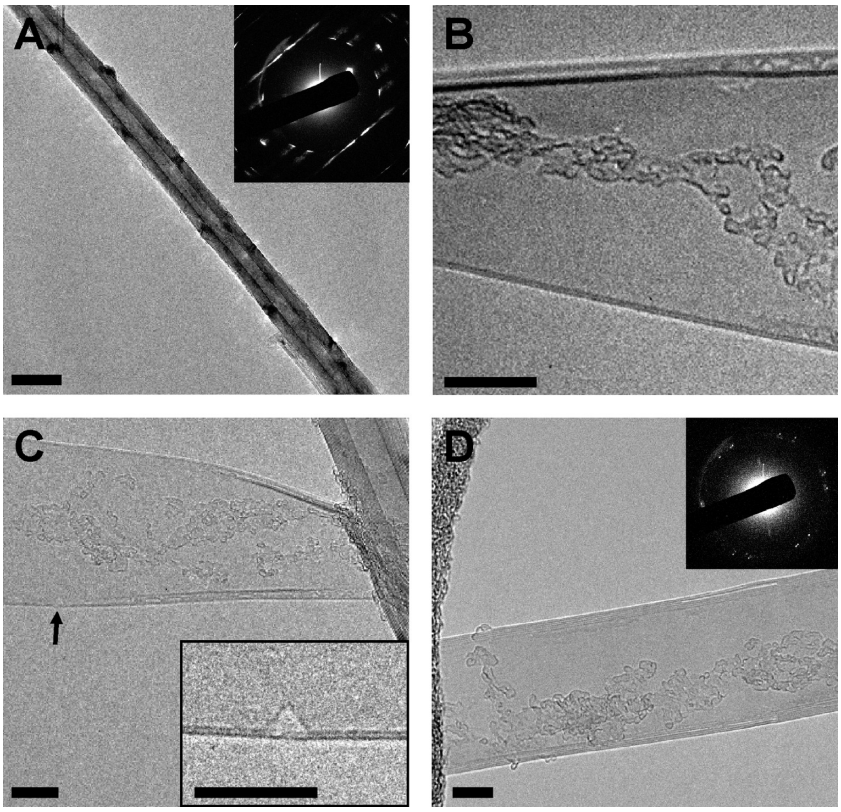

Figure 3. TEM micrographs of the following: (A) Common BNNT precursor. Scale bar is 50 nm. Inset is diffraction of the BNNT. Diffraction peaks elongate perpendicularly to the tube axis, indicating a cylindrical geometry. (B) A few layer BNNR that has a pristine, straight edge along the bottom and is scrolled at the top. Carbonaceous adsorbates are noticeable on the ribbon surface. Scale bar is 10 nm. (C) Another few layer BNNR that has unzipped off its parent tube on the right. Arrow marks the zoomed in region found in the inset, which highlights a singular triangular defect found along the ribbon edge. Scale bars are 10 nm. (D) A lone BNNR about 5 layers thick. Scale bar is 10 nm. Inset shows diffraction of BNNR which lacks elongation of diffraction peaks indicating a flat geometry.

Figure 3A displays a TEM micrograph of a typical BNNT precursor. The tube displays characteristic higher contrast walls with a lower contrast inner core.[22] The periodic darkened regions along the length of the nanotube are common for high quality BNNTs.[23] Diffraction of the BNNT (Figure 3A inset) displays spots that are elongated perpendicularly to the tube axis, owing to the curvature of the nanotube, and demonstrates high intrawall crystallinity.[23]

Figure 3B displays a TEM micrograph of a BNNR likely two layers thick with a pristine, linear edge and nearly defect-free surface. This ribbon scrolls up along the top and some carbonaceous adsorbates are noticeable on the ribbon surface. Figure 3C displays a TEM micrograph of a BNNR 40 nm in width which has been partially split off of its parent tube. This ribbon also appears to be two layers thick and scrolls up when near the parent tube, straightening out further from the tube. This ribbon also has minimal defects within the plane and along its edge, but the inset of Figure 3C highlights a singular defect found along the edge. Triangular defects like this are commonly observed when boron nitride materials are subjected to electron beam irradiation and normally a defect of this geometry is zigzag along its edge.[24] Assuming this orientation, the general ribbon edge here would be zigzag. This is likely since BNNTs often form with all their walls being mostly of armchair or mostly of zigzag orientation,[22] yielding ribbons with edges defined by the tube chirality. The periodic contrast seen along the observed edge in the micrographs of Figure 3 should not be mistaken for the ribbon edge where bond termination occurs. It instead represents a fold where the edge of the ribbon folds back onto the plane of the ribbon.[25] Such edge folding or partial scrolling is common in graphitic materials,[25,26] including GNRs,[7] and it is also observed for boron nitride materials.[18] However, the linear nature of the observed edge likely indicates a similarly straight edge where bond termination does occur.

Brief sonication in isopropanol separates many ribbons from their parent tubes, and a lone ribbon of about 5 layers is seen in Figure 3D. Diffraction of the BNNR (Figure 3D inset) is markedly different from the diffraction of a BNNT. Specifically, the curvature-induced elongation of diffraction spots, seen for nanotubes, is absent for the ribbon, indicating its flat geometry. This diffraction pattern further indicates that the highly crystalline nature of the parent BNNTs is conserved during BNNR formation. It also reveals the edge orientation to be approximately armchair in this ribbon. Although BNNRs, similar to the parent BNNTs,[22] are expected to often have successive layers of a similar orientation, our diffraction studies also show a second set of spots resulting from either another preferred orientation of some layers or folding of the ribbon along the edge.

Figure 4 shows more BNNRs that are well-separated from their parent tubes, one being at least 1 μm in length. Ribbons tend to drape along the lacey carbon and BNNTs making the full length of the ribbons difficult to determine. The flexibility of the BNNRs is evident as a ribbon changes slightly in direction while draping along the lacey carbon support in Figure 4A. Figure 4B

dx.doi.org/10.1021/nl2014857 |*Nano Lett.* XXXX, XXX, 000–000

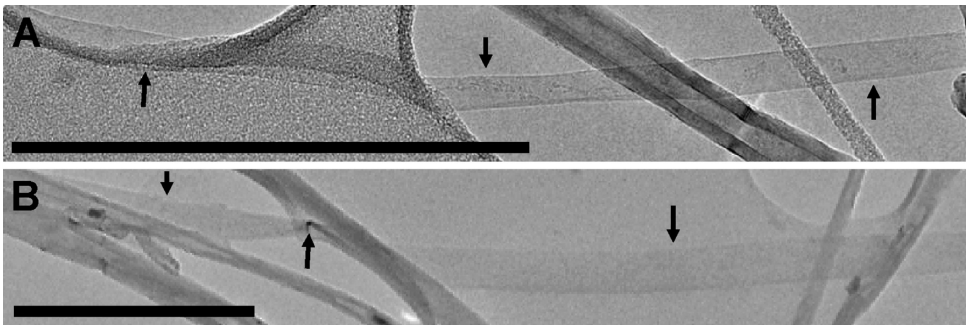

Figure 4. TEM micrographs of the following: (A) A long BNNR, having a consistent width along the length of the ribbon and straight edges. It spans across the image draping on top of lacey carbon to the left and over an unzipped BNNT to the right. Three arrows point to the ribbon to aid identification. (B) A BNNR over 1 μm in length, pointed to by the arrows. The middle arrow points to a twist in the BNNR. Scale bars in (A) and (B) are 300 nm.

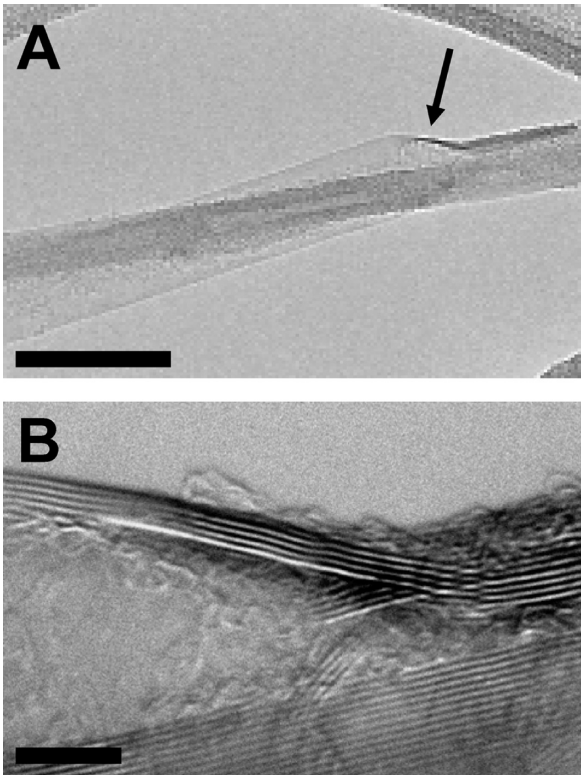

Figure 5. TEM micrographs of the following: (A) A few layer BNNR splitting off its parent ribbon. The arrow marks the zoomed in region found in (B). Scale bar is 50 nm. (B) Zoomed-in region where the few layer nanoribbon is seen coming off its parent nanotube. Scale bar is 5 nm.

shows another ribbon with a full twist (labeled by the middle arrow). Such geometries are not possible for rigid BNNTs. Ribbons are seen to have consistent widths along their entire lengths, only changing in apparent width when accommodating geometries like the twist seen in Figure 4B.

Figure 5 displays details of a ribbon in the process of splitting off its parent tube, clearly displaying how a few outer walls peel off of the nanotube to form the nanoribbon, which then separates away from the parent tube. Again, straight edges and a consistent width are observed for this ribbon. Although the intermediate stage of splitting is highlighted here, most BNNRs are seen to be fully separated from their parent BNNT following the gentle sonication used to disperse them in solution.

Potassium intercalation between walls of a nanotube is crucial for the splitting process with the previously reported GNRs synthesis[7] and is considered essential in our case of BNNR formation. However, unlike the case of graphitic materials where there exists a large body of research on intercalation compounds,[27] studies on the intercalation of *h*-BN are limited.[28,29] Alkali metals are among the few experimentally reported intercalants of *h*-BN,[28,30] and the equilibrium interplanar spacing for potassium intercalated *h*-BN has been calculated to be 5.8 Å.[31] For a nanotube, this significant increase in wall spacing from 3.4 Å[22] would result in significant bond strain circumferentially around the tube. The mechanism of splitting proposed to occur during potassium intercalation of CNTs likely also occurs for BNNTs, whereupon intercalated potassium islands grow from an initial starting point of intercalation.[7] This island growth continues until enough circumferential strain results in bond breakage. Finally, potassium bonds to the bare ribbon edge and the hindrance arising from these moieties induces further splitting longitudinally.[7] If the potassium intercalation-induced splitting of BNNTs occurred randomly within the tube, the edges of the resultant ribbons would be expected to be only moderately straight. The extremely linear, high quality edges observed for our BNNRs indicate that some further order to the splitting process occurs.

To understand the mechanism of splitting, a further look at the bonding structure of BNNTs is instructive. A significantly larger interplanar interaction exists between walls of a BNNT compared to CNT walls as polar boron−nitrogen in-plane bonds result in AA′ stacking between planes to allow heteroatoms from adjacent walls to align.[22] This often results in all walls of a BNNT being of nearly the same chirality, unlike the random chiralities found in CNTs, which maximizes the overlap between boron and nitrogen atoms in adjacent walls.[22] However, the commensurate stacking cannot continue around the full circumference of a tube given the changing diameter of concentric tube walls. A thorough TEM diffraction study[23] revealed that this geometric constraint often results in tubes that are formed in a double helical fashion. One helix consists of walls which are AA′ stacked and flat with facets along the helix. A second helix completes the tube which has consecutive walls that are mismatched and not AA′ stacked. The crystalline helix causes characteristic diffraction peaks of a faceted, polygonal structure whereas the lower crystallinity helix causes diffraction peaks characteristic of a cylindrical structure. Finally, within the highly crystalline faceted helix, lines of strained sp^3 bonds connect each facet, on the order of six facets around

dx.doi.org/10.1021/nl2014857 |*Nano Lett.* XXXX, XXX, 000–000

the tube, with these lines running parallel to the longitudinal axis of the tube.[23]

We propose that due to the observed highly linear edges of our BNNRs, potassium likely preferentially intercalates near these higher energy lines of sp^3 bonds connecting facets and eventually begins splitting along these lines. Splitting then propagates down the tube following these lines of weaker bonds, also inducing splitting through the mismatched structure regions. This splitting along predefined lines within the BNNTs explains the high quality, linear edges that are seen on the BNNRs. Also, boron atoms along these lines would be highly acidic with enhanced reactivity toward electropositive potassium, allowing for easier splitting along the lines. Furthermore, a larger interplanar spacing exists along these lines of sp^3 bonds likely allowing for more facile intercalation into these regions. Finally, intercalation likely facilitates exfoliation of unzipped walls as it disturbs the interplanar interaction between the BNNT walls. Splitting through this process should not introduce defects within the ribbon plane, as we have observed with our BNNRs. As with most nanomaterials, each particular BNNT varies significantly from the next in terms of overall structure and geometry. Therefore, although this mechanism is proposed, it is understood that the splitting to form each ribbon is highly dependent upon the particular characteristics of the parent tube and much more complex mechanics may occur to allow for each individual ribbon to form.

Since BNNTs will often form in either zigzag or armchair orientation,[22] the longitudinal splitting of BNNTs seen in this study may result in a high proportion of ribbons with zigzag and armchair edges (Figure 3) as opposed to other edge orientations. This is especially exciting given the significant body of theoretical work done on BNNRs requiring edges with minimal defects and usually of zigzag orientation.[12,13,15−17,19] Predicted properties for BNNRs include metallic or semiconducting electronic states, which can be magnetically polarized,[10,12,13,15,17,19] as well as edges displaying ferromagnetism or antiferromagnetism,[13,15,17,19] all of which are dependent upon edge geometry and termination. Given this significant dependence upon BNNR edges for imbuing particular electronic and magnetic properties, the high likelihood of synthesizing ribbons with zigzag edges may make them particularly suitable for addressing theoretical predictions and realizing proposed applications. It is also worthwhile to consider the possibility of functionalizing the edges of these BNNRs. GNR edges synthesized via this route are potassium terminated during synthesis and hydrogen terminated upon exposure to water or ethanol.[7] BNNRs synthesized through this route could be similarly terminated, and many of the predicted BNNR properties necessitate hydrogen-terminated edges.[13,15−17,19] Furthermore, the reactive potassium-terminated edge could easily be replaced with species other than hydrogen. Different chemicals could be used for quenching to impart other terminations. In addition, hydrogen could be replaced after quenching by either utilizing established boron nitride functionalization routes[32,33] or by devising new routes unique to the highly reactive nanoribbon edge.

■ ASSOCIATED CONTENT

Supporting Information. Micrograph of BNNTs, experimental details, and information regarding model generation. This material is available free of charge via the Internet at http://pubs.acs.org.

■ AUTHOR INFORMATION

Corresponding Author

*E-mail: (A.K.Z.) azettl@berkeley.edu; (J.M.T.) tour@rice.edu.

■ ACKNOWLEDGMENT

This work was supported in part by the Director, Office of Science, Office of Basic Energy Sciences, Division of Materials Sciences and Engineering, of the U.S. Department of Energy under Contract No. DE-AC02-05CH11231 which provided for BNNT synthesis and preliminary intercalation via the sp^2 and Hydrogen programs. The Center of Integrated Nanomechanical Systems (COINS) with NSF Grant EEC-0425914 provided support for TEM imaging. The Office of Naval Research MURI Graphene Program provided support for sample characterization and modeling. A.S. and J.M.T. further acknowledge the support by the Air Force Research Laboratory through University Technology Corporation, 09-S568-064-01-C1, and the Air Force Office of Scientific Research FA9550-09-1-0581.

■ REFERENCES

(1) Iijima, S. *Nature* **1991**, *354* (6348), 56–58.
(2) Novoselov, K. S.; Geim, A. K.; Morozov, S. V.; Jiang, D.; Zhang, Y.; Dubonos, S. V.; Grigorieva, I. V.; Firsov, A. A. *Science* **2004**, *306* (5696), 666–669.
(3) Geim, A. K.; Novoselov, K. S. *Nat. Mater.* **2007**, *6* (3), 183–191.
(4) Jiao, L.; Wang, X.; Diankov, G.; Wang, H.; Dai, H. *Nat. Nanotechnology* **2010**, *5* (5), 321–325.
(5) Jiao, L.; Zhang, L.; Wang, X.; Diankov, G.; Dai, H. *Nature* **2009**, *458* (7240), 877–880.
(6) Kosynkin, D. V.; Higginbotham, A. L.; Sinitskii, A.; Lomeda, J. R.; Dimiev, A.; Price, B. K.; Tour, J. M. *Nature* **2009**, *458* (7240), 872–876.
(7) Kosynkin, D. V.; Lu, W.; Sinitskii, A.; Pera, G.; Sun, Z.; Tour, J. M. *ACS Nano* **2011**, *5* (2), 968–974.
(8) Chopra, N. G.; Luyken, R. J.; Cherrey, K.; Crespi, V. H.; Cohen, M. L.; Louie, S. G.; Zettl, A. *Science* **1995**, *269* (5226), 966–967.
(9) Nagashima, A.; Tejima, N.; Gamou, Y.; Kawai, T.; Oshima, C. *Phys. Rev. B* **1995**, *51* (7), 4606.
(10) Azadi, S.; Moradian, R. *Phys. Lett. A* **2010**, *374* (4), 605–609.
(11) Barone, V.; Peralta, J. E. *Nano Lett.* **2008**, *8* (8), 2210–2214.
(12) Chen, W.; Li, Y.; Yu, G.; Li, C.-Z.; Zhang, S. B.; Zhou, Z.; Chen, Z. *J. Am. Chem. Soc.* **2010**, *132* (5), 1699–1705.
(13) Ding, Y.; Wang, Y.; Ni, J. *Appl. Phys. Lett.* **2009**, *94* (23), 233107–3.
(14) Feng, C.; Yuan-Ping, C.; Mi, Z.; Jian-Xin, Z. *Chin. Phys. B* **2010**, *19* (8), 086105.
(15) Lai, L.; Lu, J.; Wang, L.; Luo, G.; Zhou, J.; Qin, R.; Gao, Z.; Mei, W. N. *J. Phys. Chem. C* **2009**, *113* (6), 2273–2276.
(16) Park, C.-H.; Louie, S. G. *Nano Lett.* **2008**, *8* (8), 2200–2203.
(17) Topsakal, M.; Akturk, E.; Ciraci, S. *Phys. Rev. B* **2009**, *79* (11), 115442.
(18) Zeng, H.; Zhi, C.; Zhang, Z.; Wei, X.; Wang, X.; Guo, W.; Bando, Y.; Golberg, D. *Nano Lett.* **2010**, *10* (12), 5049–5055.
(19) Zheng, F.; Zhou, G.; Liu, Z.; Wu, J.; Duan, W.; Gu, B.-L.; Zhang, S. B. *Phys. Rev. B* **2008**, *78* (20), 205415.
(20) Sinitskii, A.; Dimiev, A.; Kosynkin, D. V.; Tour, J. M. *ACS Nano* **2010**, *4* (9), 5405–5413.
(21) Zhi, C.; Bando, Y.; Tan, C.; Golberg, D. *Solid State Commun.* **2005**, *135* (1−2), 67–70.
(22) Golberg, D.; Bando, Y.; Tang, C. C.; Zhi, C. Y. *Adv. Mater.* **2007**, *19* (18), 2413–2432.
(23) Celik-Aktas, A.; Zuo, J. M.; Stubbins, J. F.; Tang, C. C.; Bando, Y. *Acta Crystallogr., Sect. A* **2005**, *61*, 533–541.

(24) Alem, N.; Erni, R.; Kisielowski, C.; Rossell, M. D.; Gannett, W.; Zettl, A. *Phys. Rev. B* **2009**, *80* (15), 155425.
(25) Zhang, J.; Xiao, J.; Meng, X.; Monroe, C.; Huang, Y.; Zuo, J.-M. *Phys. Rev. Lett.* **2010**, *104* (16), 166805.
(26) Rotkin, S. V.; Gogotsi, Y. *Mater. Res. Innovations* **2002**, *5* (5), 191–200.
(27) Dresselhaus, M. S.; Dresselhaus, G. *Adv. Phys.* **2002**, *51* (1), 1–186.
(28) Doll, G. L.; Speck, J. S.; Dresselhaus, G.; Dresselhaus, M. S.; Nakamura, K.; Tanuma, S. I. *J. Appl. Phys.* **1989**, *66* (6), 2554–2558.
(29) Shen, C.; Mayorga, S. G.; Biagioni, R.; Piskoti, C.; Ishigami, M.; Zettl, A.; Bartlett, N. *J. Solid State Chem.* **1999**, *147* (1), 74–81.
(30) Sumiyoshi, A.; Hyodo, H.; Kimura, K. *J. Phys. Chem. Solids* **2010**, *71* (4), 569–571.
(31) Okada, S.; Otani, M. *Phys. Rev. B* **2010**, *81* (23), 233401.
(32) Ikuno, T.; Sainsbury, T.; Okawa, D.; Fréchet, J. M. J.; Zettl, A. *Solid State Commun.* **2007**, *142* (11), 643–646.
(33) Zhi, C. Y.; Bando, Y.; Terao, T.; Tang, C. C.; Kuwahara, H.; Golberg, D. *Chem.—Asian J.* **2009**, *4* (10), 1536–1540.

dx.doi.org/10.1021/nl2014857 |*Nano Lett.* XXXX, XXX, 000–000